

Research Article

Preparation, Encapsulation, and Performance Evaluation of Ternary Phase Change Materials for Building Envelope

Hongzhi Zhu, Bin Guo , and Zhi Li

College of Hydraulic and Civil Engineering, Shandong Agricultural University, Tai'an 271018, Shandong, China

Correspondence should be addressed to Bin Guo; guobin@sdau.edu.cn

Received 27 November 2021; Revised 16 March 2022; Accepted 18 March 2022; Published 1 April 2022

Academic Editor: Guoming Liu

Copyright © 2022 Hongzhi Zhu et al. This is an open access article distributed under the Creative Commons Attribution License, which permits unrestricted use, distribution, and reproduction in any medium, provided the original work is properly cited.

Background. In order to make up for the defect that a single phase change material cannot meet the phase change temperature in a specific application field, three kinds of materials with higher phase change temperature are selected in this paper. Through the phase change material composite method, it was adopted to carry out step cooling curve test and differential scanning calorimetry (DSC) test, based on the second law of thermodynamics and the theory of phase equilibrium. DSC thermal analysis and Fourier transform infrared spectroscopy (FT-IR) characterization were carried out. The phase change diatomite was used for packaging materials and durability evaluation. The results show that when TD-MA : LA = 6.2 : 3.8, the phase transition temperature of the experimental ternary composite phase change material is 20.1°C. The adsorption of diatomite to phase change material (PCM) is only physical adsorption, and the thermal stability is good after 100 phase change cycles. The maximum mass loss rate of phase change diatomite encapsulated by phenylpropene emulsion and cement powder is only 0.65%, at last, this phase change diatomite is suitable for building envelope structure.

1. Introduction

Phase change heat storage technology is a method for energy storage by using the characteristics of phase change materials (PCMs) that can absorb or release a large amount of phase change latent heat during phase change [1]. Phase change materials are used in building envelopes to strengthen the heat preservation, heat storage, and heat insulation capabilities of the envelope structure, thus can reduce heating and air conditioning energy consumption, reduce electrical load, and ultimately achieve energy saving goals [2–7].

A single phase change material is sometimes difficult to meet the requirements of a certain field for the phase change temperature and phase change materials. Therefore, many scholars prepare composite phase change materials with the required phase change temperature by mixing two or more phase change materials [8–12]. However, there are few studies on the preparation of ternary composite phase change materials to improve the utilization rate of phase change materials. The phase change material usually needs to

be shaped and packaged before it is put into use, so as to make up for its shortcomings of low thermal conductivity such as large volume change during phase change and easy leakage. Commonly used encapsulation methods include methods of porous carriers composite, macro encapsulation, sol-gel encapsulation, microcapsule encapsulation, etc. [13–16]. C. Hasse et al. prepared phase change paraffin microcapsules and encapsulated them in the honey comb panel [17]. The experiment found no phase change material leakage in the panel. Ramakrishnan S prepared a composite phase change material with paraffin wax and expanded perlite as raw materials in which mass ratio of paraffin can reach 50% [18, 19] the experimental results show that the composite PCM has good chemical compatibility and thermal stability. Although these methods have many advantages, secondary encapsulation is still needed to improve the stability of phase change materials in the phase change cycle.

This paper aims to prepare and select ternary composite phase change materials suitable for building envelopes by using phase change materials TD, MA, LA as raw materials,

using the method of heating and melting and processing cooling curve and DSC test. Using diatomaceous Earth as a matrix to shape the phase change material and encapsulate it with a packaging material, illustrating the FT-IR characterization of the phase change material and the shaped phase change material.

2. Experiment

2.1. Experimental Materials and Instruments. Tetradecanol (TD), called myristyl alcohol, is a colorless to white waxy solid. Myristic acid (MA), a white crystalline waxy solid. Lauric acid (LA), called dodecanoic acid, a white flake or bead-like solid. The particle size of Expanded perlite (EP) is between 2 mm to 3 mm, appearing white particles, honeycomb pore structure. The particle size of diatomite (DE) is between 5 mm and 15 mm, appearing white or light yellow particles. Styrene acrylic emulsion is a thick milky liquid. Cement powder (wet with water). Magnetic heating stirrer, electronic balance, temperature acquisition instrument, temperature sensor, differential scanning calorimeter (DSC), Fourier transform infrared spectrometer (FT-IR), vacuum drying oven, refrigerated refrigerator.

2.2. Experimental Procedures and Methods

2.2.1. Theoretical Prediction of Thermophysical Properties of Ternary Composite Phase Change Materials. According to the second law of thermodynamics and phase equilibrium theory, the melting point and heat of solution formula of the eutectic phase change material can be obtained, so as to theoretically predict the eutectic temperature of the eutectic system and the proportion of corresponding components. The eutectic temperature formula and the heat of solution formula of the binary composite phase change material are as follows.

$$T_m = \frac{1}{1/T_A - R \ln X_A/H_A} \quad (1)$$

$$= \frac{1}{1/T_B - R \ln X_B/H_B},$$

$$H_m = T_m \left[\frac{X_A H_A}{T_A} + \frac{X_B H_B}{T_B} \right], \quad (2)$$

$$X_A + X_B = 1. \quad (3)$$

Among them, T_m is the melting temperature of the eutectic phase change material, K. H_m is the heat of fusion of the eutectic phase change material, J/mol, T_A , T_B , are the melting temperatures of the A and B components respectively, K. H_A , H_B , are the latent heat of phase change of A and B components, J/mol. X_A , X_B are the mole percentages of A and B components in the mixture, respectively.

In the calculation, the thermal properties of TD and MA are first brought into the above formulas (1)–(3), contributing to the eutectic point temperature of the TD-MA binary

eutectic is 304 K and the heat of solution is 198 J. Converting the calculated mole percentage to mass percentage is TD: MA = 67.4:32.6, and the TD-MA binary eutectic is combined with LA as a single component. When the mass ratio TD-MA:LA = 62.5:37.5, the eutectic point temperature of the TD-MA-LA eutectic is 295.2 K, which meets the temperature requirements of the building envelope for phase change materials.

2.2.2. Step Cooling Curve Test of Composite Phase Change Materials. In this experiment, the TD-MA binary composite phase change material is set to 9 different mass ratios (8:2, 7:3, 6:4, 4:6, 2:8), (6.8:3.2, 6.7:3.3, 6.6:3.4, 6.5:3.5) Perform step cooling curve test. Compound the obtained TD-MA binary eutectic compound with LA, and set TD-MA:LA to 6 different mass ratios (8:2, 6.3:3.7, 6.2:3.8, 6.1:3.9, 6:4, 4:6, 2:8) Continue the experiment, after that, DSC test was combined for analysis and comparison.

2.2.3. DSC Test of Composite Phase Change Material. The phase change temperature and latent heat of the composite phase change materials with different proportions were obtained by DSC test using differential scanning calorimetry.

2.2.4. Performance Characterization of Shaped Composite Phase Change Materials. The amorphous phase change materials were prepared by using diatomite as the matrix adsorption phase change material. The amorphous phase change materials before and after the phase change cycle were tested by differential scanning calorimetry. The chemical composition and structure of the fixed phase change materials before and after phase change cycle were analyzed by Fourier transform infrared absorption spectrometer.

2.2.5. Shaped Composite Phase Change Material Packaging and Durability Test. Weighing 4 parts of 20 g phase change diatomaceous Earth shaped composite phase change material, one of which is not packaged, and the other three are packaged in different packaging methods, and the thermal cycle test is performed on them, and the different packaging is evaluated by the mass loss rate cold and hot cycle durability under the material.

3. Results and Analysis

3.1. Step Cold Curve Test and Analysis. Using the SRND-CM-4PT distributed modular automatic measuring unit to perform step-cooling temperature curve test on TD-MA binary composite phase change materials and TD-MA-LA ternary composite phase change materials with different mass ratios, and collect temperature data after temperature data is collected, the time-temperature curve is drawn as shown in Figures 1–3.

It can be seen from Figure 1 that the TD-MA curve under different ratios has a transition under different mass ratios,

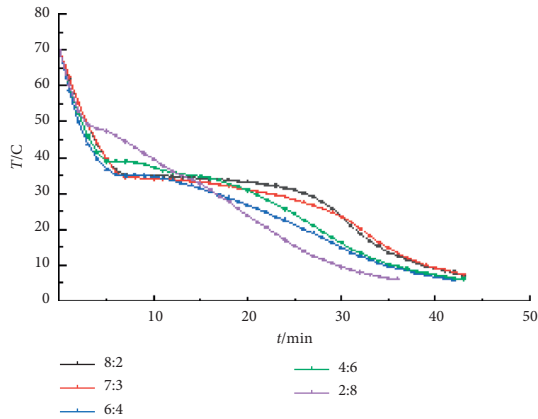


FIGURE 1: Step cooling curve of TD-MA binary composite phase change materials under different mass ratios.

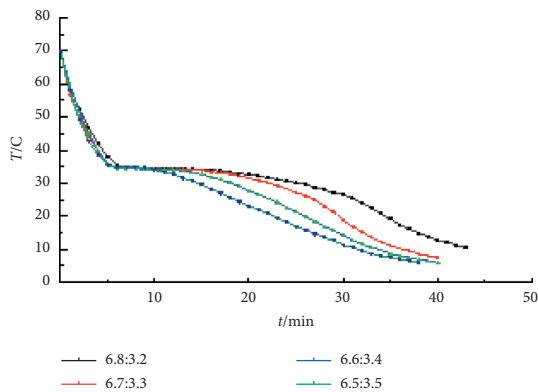


FIGURE 2: Step cooling curve of TD-MA binary composite phase change materials with different mass ratios near eutectic point.

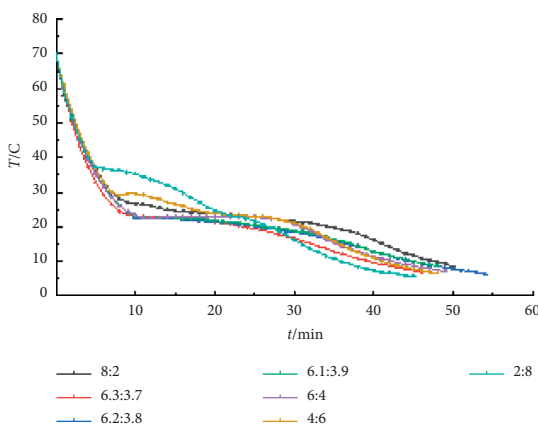


FIGURE 3: Step cooling curves of binary eutectic TD-MA and LA at different mass ratios.

indicating that the TD-MA composite phase change materials under different mass ratios have crystallized during the cooling process. Moreover, the size of the temperature plateau is different, indicating that the size of the latent heat of phase change is different. When the mass ratio TD : MA is 8 : 2, 7 : 3, 6 : 4, 4 : 6, 2 : 8, the crystallization temperature is 35.3°C, 34.7°C, 35°C, 38.7°C, and 49.0°C, respectively. The

crystallization temperature is lower at 7 : 3 and 6 : 4, and it is preliminarily judged that the eutectic point temperature appears between these two ratios.

Figure 2 shows the step cooling curves of TD-MA composite phase change materials with different ratios near the low eutectic point. It can be seen that the TD-MA composite phase change materials under the four mass ratios have crystallized during the cooling process. When the mass ratio is 6.5 : 3.5, the crystallization temperature is slightly higher and the phase transition duration is shorter, so it is excluded. The crystallization temperature of the other three ratios is close, and it is not easy to distinguish in the step cooling curve, so take these three ratios to continue the DSC test.

It can be seen from Figure 3 that the binary eutectic TD-MA and LA at different mass ratios of TD-MA-LA ternary composite phase change materials have crystallized during the cooling process. When the mass ratio TD-MA : LA is 8 : 2, 6 : 4, 4 : 6, 2 : 8, the crystallization temperature is 27.2°C, 24.4°C, 29.6°C, and 37.3°C, respectively. When the mass ratio is near the theoretically predicted eutectic point mass ratio, the crystallization temperature is the lowest and the crystallization temperature is within the comfortable temperature of the human body, roughly between 20°C and 25°C, but the difference is small and difficult to distinguish, so take TD-MA. The ratio of LA was tested by DSC at 6.3 : 3.7, 6.2 : 3.8, 6.1 : 3.9.

3.2. DSC Test Analysis of Composite Phase Change Materials.

The DSC test curves of the TD-MA binary composite phase change material near the mass ratio of the eutectic point predicted by theory are shown in Figures 4–6. The DSC test curves of the TD-MA-LA ternary composite phase change material near the mass ratio of the eutectic point predicted by theory are shown in Figures 7–9.

From Figures 4–6, it can be concluded that when the mass ratio TD : MA is 6.8 : 3.2, 6.7 : 3.3, 6.6 : 3.4, the phase transition temperature of the TD : MA binary composite phase change material is 33.4°C, 33.1°C, and 34.8°C. When the ratio of the two is 6.7 : 3.3, the TD-MA binary composite phase change material has a low eutectic point, which is 1.1°C different from the theoretical prediction, and the latent heat of phase change is 208.3 J/g, which is closed to the theoretical prediction. Therefore, take this ratio of TD-MA binary composite phase change material to continue the configuration of ternary composite phase change material.

It can be seen from Figures 7–9 that the phase transition temperature of the TD-MA-LA ternary composite phase change material with the mass ratio near the eutectic point is predicted to be around 20°C. The ternary composite phase change material when TD-MA : LA = 6.2 : 3.8 is selected as the final material required for this study. The phase change temperature is 20.1°C, and the latent heat of phase change is larger, which is 154.6 J/g. Compared with other ratios, TD-MA : LA = 6.2 : 3.8 has great advantages, suitable phase change temperature and large latent heat of phase change, which can satisfy the building envelope structure.

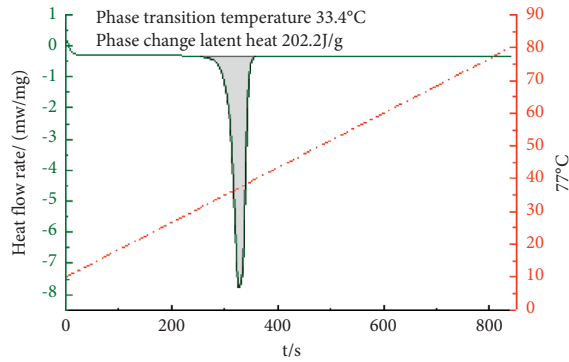


FIGURE 4: TD:MA is the DSC curve of TD-MA at 6.8:3.2.

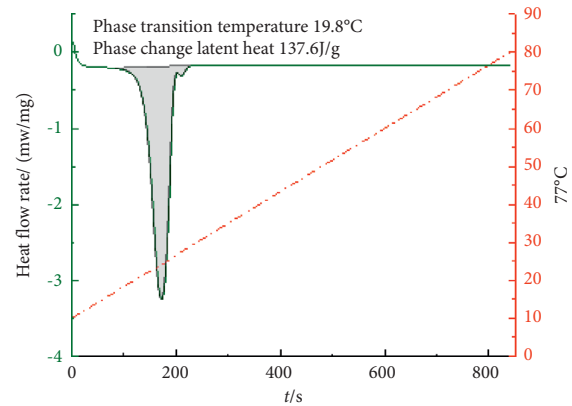


FIGURE 7: TD-MA:LA is the DSC curve of TD-MA-LA at 6.3:3.7.

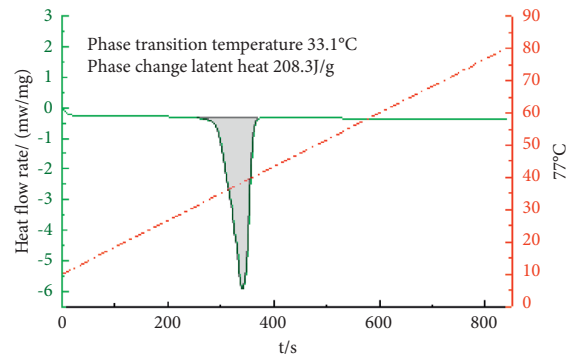


FIGURE 5: TD:MA is the DSC curve of TD-MA at 6.7:3.3.

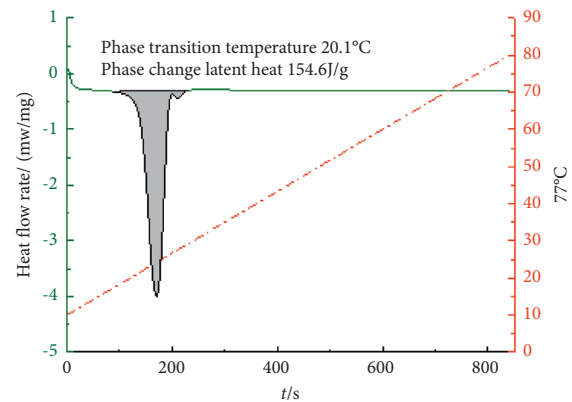


FIGURE 8: TD-MA:LA is the DSC curve of TD-MA-LA at 6.2:3.8.

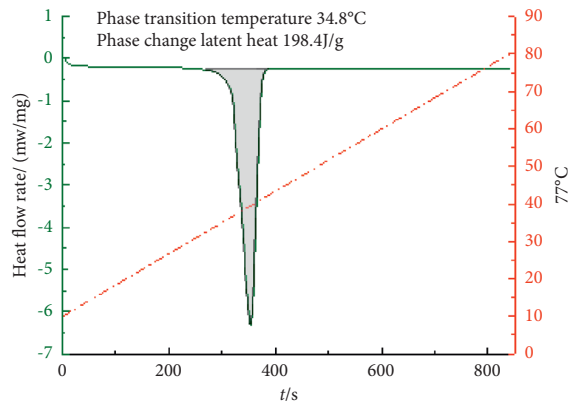


FIGURE 6: TD:MA is the DSC curve of TD-MA at 6.6:3.4.

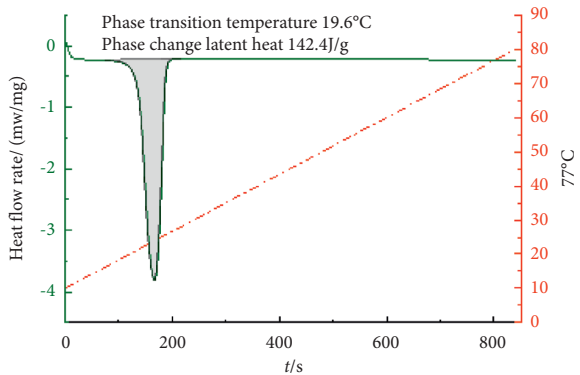


FIGURE 9: TD-MA:LA is the DSC curve of TD-MA-LA at 6.1:3.9.

3.3. FT-IR Analysis. The infrared spectra of LA, MA, TD, and TD-MA-LA eutectics measured experimentally are as shown in Figure 10. The infrared spectra of TD-MA-LA eutectic, diatomaceous Earth, and phase change diatomite are showed in Figure 11.

From Figure 10, it can be seen that the positions of the peaks in the infrared spectra of LA and MA and their strengths are similar. Observe the infrared spectra of LA. There are two characteristic absorption peaks at 2920 cm^{-1} and 2840 cm^{-1} , respectively, which are CH_3 -symmetrical stretching vibration peak, $-\text{CH}_2$ -Asymmetrical stretching vibration peak. The $\text{C}=\text{O}$ stretching vibration absorption peak appears at 1700 cm^{-1} , the $-\text{CH}_2$ - flexural vibration peak

appears at 1470 cm^{-1} , and the OH surface deformation flexural vibration peak appears at 1415 cm^{-1} . At 930 cm^{-1} and 725 cm^{-1} , the bending vibration peaks of the terminal alkenyl group CH and the $(\text{CH}_2)_{10}$ bending vibration absorption peaks appear. Observe the infrared spectrum curve of TD, the peak at 3332 cm^{-1} is the characteristic absorption peak of the OH bond vibration of alcohol and water molecules. The spectrum shows CH_3 -symmetric stretching vibration peaks and $-\text{CH}_2$ -asymmetry at 2920 cm^{-1} and

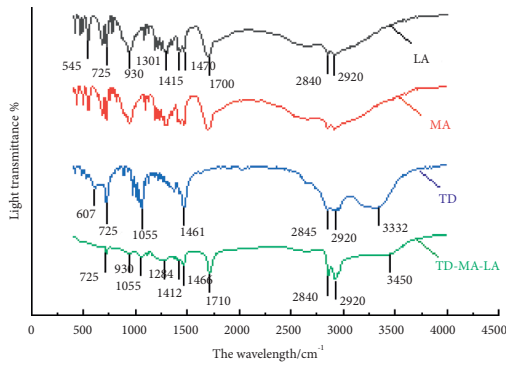


FIGURE 10: Infrared spectra of La, Ma, Td, and TD-MA-LA composite phase change materials/.

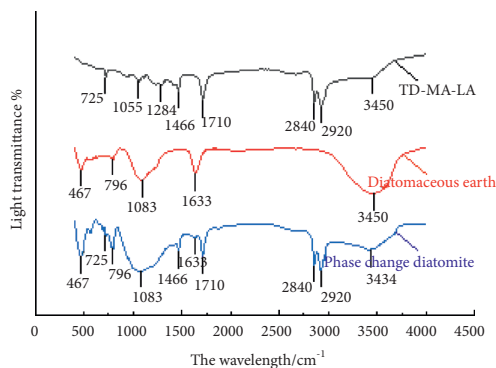


FIGURE 11: Spectrum of TD-MA-LA eutectic, diatomite and phase change diatomite.

2845 cm^{-1} . Stretching vibration peak, the peak at 1461 cm^{-1} is $-\text{CH}_2-$ flexural vibration peak, and the peak at 1055 cm^{-1} is CO stretching vibration absorption peak. Compared with the infrared spectra of LA and TD, the infrared spectra of TD-MA-LA can be seen at 3450 cm^{-1} , 2920 cm^{-1} , 2840 cm^{-1} , 1710 cm^{-1} , 1464 cm^{-1} , 1412 cm^{-1} , 1055 cm^{-1} , and 930 cm^{-1} . Corresponding characteristic absorption peaks also appeared at 725 cm^{-1} , and no new characteristic peaks were generated. Only the position of individual peaks has a slight deviation and the strength of some peaks has changed slightly, indicating that the ternary composite phase change material is only physically mixed during the preparation process, and no chemical reaction occurs.

It can be seen from Figure 11 that the O-H bond of water molecules and the Si-O-H bond stretching vibration absorption peak of diatomite appear at 3450 cm^{-1} of diatomite. Corresponding to the O-H bending vibration peak at 1633 cm^{-1} , the characteristic absorption peak at 1083 cm^{-1} is the cyclic Si-O-Si stretching vibration absorption peak, and the Si-O bending vibration absorption peak at 467 cm^{-1} . It can be seen from the infrared spectrum of the phase change diatomite that it contains all the characteristic peaks of diatomite and TD-MA-LA composite materials, and no new characteristic peaks are generated, indicating that the phase change diatomite is in the preparation only physical adsorption, no chemical reaction occurs.

3.4. DSC Characterization of Shaped Composite Phase Change Materials. The DSC curves of TD-MA-LA and phase change diatomite before and after cycling are shown in Figure 12.

It can be seen from Figure 12 that the phase change temperature of the phase change diatomite after the adsorption of the phase change material by diatomite is 20.4°C , which is 0.3°C change from previous adsorption, and the latent heat of phase change appears to be reduced to 55.9 J/g . The phase change temperature of the phase change diatomite after 100 cycles of phase change is 20.3°C , which is a change of 0.1°C from before the cycle, and the latent heat of phase change is 51.2 J/g , which is 8.4% lower than that before the cycle, showing that phase change diatomite has good thermal stability.

3.5. Analysis of Durability Results of Cooling and Heating Cycles. The mass of phase-change diatomite after encapsulation by styrene-acrylic emulsion, cement powder, styrene-acrylic emulsion+cement powder is 39.52 g , 39.27 g , and 49.61 g , respectively, and the durability of phase-change diatomaceous Earth under different packaging methods. And the test results are shown in Table 1 and Figure 13.

It can be seen from Figure 13 that the mass loss rate of phase change diatomite under the four encapsulation methods increases with the increase of the number of phase change cycles. In the unencapsulated state, the mass loss of phase change diatomaceous Earth is relatively large, and the quality is stable after about 40 phase change cycles, and the mass loss rate is about 5.1% . The effect of packaging with cement powder and styrene-acrylic emulsion is obvious, and the maximum mass loss rate About 2.1% and 1.8% respectively. It can be seen that the encapsulation method using styrene-acrylic emulsion mixed with cement powder has the best effect. The quality is close to stable after the phase change cycle is about 20 times, and the maximum mass loss rate is only about 0.65% . From experiments that the encapsulation method of styrene-acrylic emulsion and cement powder has the best durability. It can be used with building with long service life. This encapsulation method can be used to prepare phase-change energy storage aggregates and combine with building materials to prepare phase-change energy storage concrete for use in building envelopes.

4. Discussion

To make more of the phase change materials in different areas to get reasonable application more effectively, most scholars [20] will be focused on two or more composite phase change materials, in line with the principle of phase change materials of high utilization rate, this study selected three kinds of high phase transition temperature of solid liquid phase change materials for building palisade structure after through distribution, through the theoretical prediction and experimental verification, The thermal properties of the ternary composite phase change material finally

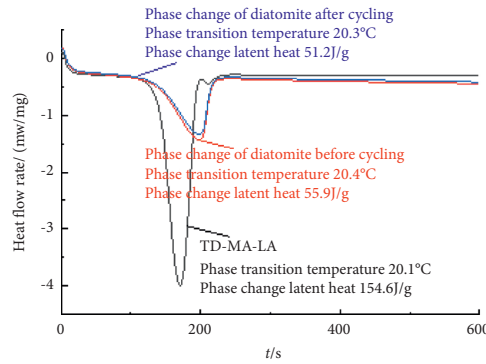


FIGURE 12: DSC curves of TD-MA-LA and phase change diatomite.

TABLE 1: Changes of mass and loss rate of phase change expanded perlite under different encapsulation methods.

Packaging materials	Cycle number	Mass/g					
		0	10	20	30	40	50
Unencapsulate	Mass/g	20.00	19.73	19.37	19.12	18.98	18.98
	Loss rate/%	0	1.4	3.2	4.4	5.1	5.1
Styrene-acrylic emulsion	Mass/g	39.52	39.34	39.24	39.16	39.16	39.16
	Loss rate/%	0	0.9	1.7	1.8	1.8	1.8
Cement powder	Mass/g	39.27	39.05	38.95	38.87	38.85	38.85
	Loss rate/%	0	1.1	1.6	2.0	2.1	2.1
Styrene-acrylic emulsion and cement powder	Mass/g	49.61	49.52	49.49	49.48	49.48	49.48
	Loss rate/%	0	0.44	0.60	0.65	0.65	0.65

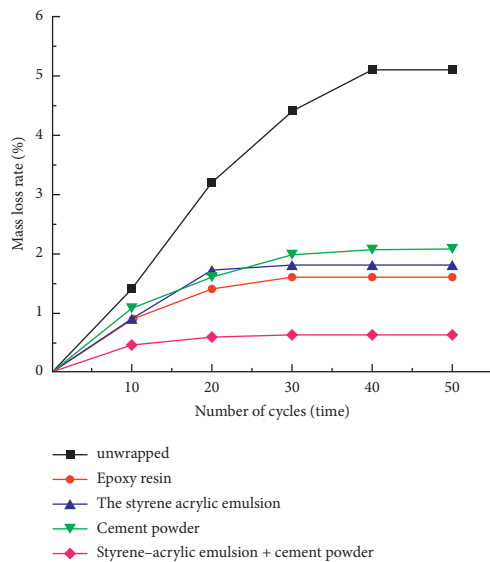


FIGURE 13: Mass loss rate of phase change expanded perlite under different encapsulation methods.

prepared meet the requirements of this study, so that the single phase change material can be reasonably utilized.

The latent heat of phase-change materials will inevitably decrease after being adsorbed by diatomite, and no new materials will be formed in the melting composite process of phase-change materials and the adsorption process of diatomite, which indicates that no chemical reaction takes

place in each component. The prepared phase-change energy storage aggregate has excellent phase-change stability. Some scholars [21–23] found that, after packaging the porous matrix material after adsorption of PCM, the leakage problem of liquid PCM would be greatly improved due to the obstruction of packaging layer on the liquid PCM. In this study, the double-packaging effect of styrene-acrylic emulsion + cement powder was very excellent. After about 10 phase transformation cycles, there was no leakage and the mass loss rate was only 0.65%. However, the problem of low adsorption rate of diatomite itself needed further study. It can be seen that how to use more phase change materials in a better way under the premise of ensuring no leakage, so as to play a greater role in phase change heat storage and release is particularly critical.

5. Conclusions

- (1) Theoretical calculation of the ternary composite phase change material TD-MA : LA = 62.5 : 37.5, the system has a eutectic point, and the eutectic point temperature is 23.2°C. Through the step cooling curve test and DSC test experiment, when TD-MA : LA = 6.2 : 3.8, the phase change temperature of the ternary composite phase change material is 20.1°C, and the latent heat of phase change is 154.6 J/g. The thermophysical properties of the final ternary composite phase change material meet the requirements for application in building envelopes.

- (2) TD, MA, LA did not undergo chemical reaction during the melting and compounding process, only physical melting and mixing. The adsorption of diatomite to the TD-MA-LA composite phase change material is only physical adsorption, and no new substances are produced during the process. The phase change latent heat of the adsorbed phase change diatomite is reduced to a certain extent, which is 55.9 J/g. The phase change temperature of diatomite is basically unchanged after the phase change cycle, the latent heat of phase change is reduced by 8.4%, and it has good thermal stability.
- (3) The cold and heat cycle durability of phase change diatomaceous Earth after encapsulation is significantly better than before encapsulation. Among them, the encapsulation method of styrene-acrylic emulsion mixed cement powder is the most excellent, with a maximum mass loss rate of only 0.65% and excellent durability.

Data Availability

The data that support the finding of this study are available from the corresponding author upon reasonable request.

Conflicts of Interest

The authors declare that they have no conflicts of interest.

References

- [1] A. S. Manirathnam, M. K. Dhanush Manikandan, R. Hari Prakash, B. K. Kumar, and M. D. Amarnath, "Experimental analysis on solar water heater integrated with Nano composite phase change material," *Materials Today Proceedings*, vol. 9, no. 1, pp. 869–921, 2020.
- [2] Y. Liu, L. Hou, Y. Yang, Y. Feng, and L. Yang, "Effects of external insulation component on thermal performance of a Trombe wall with phase change materials," *Solar Energy*, vol. 204, pp. 115–133, 2020.
- [3] J. F. Lin, "Application research of phase change materials in building Energy conservation," *Neijiang science and technology*, vol. 40, no. 4, pp. 52–53, 2019.
- [4] K. Ahmet, "Energy storage applications in greenhouses by means of phase change materials (PCMs): a review," *Renewable Energy*, vol. 13, no. 1, pp. 89–103, 1998.
- [5] T. T. Shi, X. G. Zhang, J. X. Qiao et al., "Preparation and characterization of composite phase change materials based on paraffin and carbon foams derived from starch," *Polymer*, vol. 1, pp. 123–143, 2020.
- [6] X. L. Wang, X. Cheng, D. Li et al., "Preparation a three-dimensional hierarchical graphene/stearic acid as a phase change materials for thermal energy storage," *Materials Research Express*, vol. 7, no. 9, pp. 55–60, 2020.
- [7] K. Cellat, B. Beyhan, C. Gungor et al., "Thermal enhancement of concrete by adding bio-based fatty acids as phase change materials," *Energy and Buildings*, vol. 106, no. 1, pp. 156–163, 2015.
- [8] S. L. Zhang, F. F. Chen, W. Q. Pan, S. Wang, Y. Jiang, and D. Yuan, "Development of heat transfer enhancement of a novel composite phase change material with adjustable phase change temperature," *Solar Energy Materials and Solar Cells*, vol. 210, 2020.
- [9] D. H. Jiang, X. L. Zhang, S. X. Liao, H. Fei, and Q. J. Gu, "Preparation and thermal properties of hexadecanoic acid-tetradecanol binary phase change materials," *Modern Chemical Industry*, vol. 39, no. 10, pp. 146–149, 2019.
- [10] K. Yang, M. Jiao, S. Wang, Y. Yu, D. Quan, and J. Cao, "Thermoregulation properties of composite phase change materials in high temperature environmental conditions," *International Journal of Clothing Science & Technology*, vol. 30, no. 4, pp. 507–516, 2018.
- [11] L. Gao, X. G. Sun, B. Z. Sun, D. Y. Che, and Z. Z. Liu, "Preparation and thermal properties of palmitic acid/expanded graphite/carbon fiber composite phase change materials for thermal energy storage," *Journal of Thermal Analysis and Calorimetry*, vol. 114, pp. 1–11, 2019.
- [12] P. M. Hou, J. F. Mao, R. R. Liu, F. Chen, Y. Li, and C. Xu, "Improvement in thermodynamic characteristics of sodium acetate trihydrate composite phase change material with expanded graphite," *Journal of Thermal Analysis and Calorimetry*, vol. 137, no. 4, pp. 1295–1306, 2019.
- [13] R. A. Mitran, D. Lincu, L. Buhăleanu, D. Berger, and C. Matei, "Shape-stabilized phase change materials using molten NaNO₃-KNO₃ eutectic and mesoporous silica matrices," *Solar Energy Materials and Solar Cells*, vol. 215, 2020.
- [14] T. Shi, Y. Fang, and H. X. Zhang, "Advances in the study of formalized phase change materials," *Materials bulletin*, vol. 29, no. 2, pp. 439–442, 2015.
- [15] C. Hasse, M. Grenet, A. Bontemps, R. Dendievel, and H. Sallee, "Realization, test and modelling of honeycomb wallboards containing a Phase Change Material," *Energy&Building*, vol. 43, no. 1, pp. 232–238, 2010.
- [16] S. Ramakrishnan, X. M. Wang, S. Jay, E. Petinakis, and J. Wilson, "Development of thermal energy storage cementitious composites (TESC) containing a novel paraffin/hydrophobic expanded perlite composite phase change material," *Solar Energy*, vol. 158, pp. 626–635, 2017.
- [17] W. W. Wang, X. F. Song, and Y. N. Cai, "Preparation and thermal properties of ternary fatty acid eutectic/Silicon dioxide phase change composites," *Journal of Materials Science and Engineering*, vol. 38, no. 1, pp. 68–73, 2020.
- [18] C. Li, L. Qi, and Y. L. Ding, "Carbonate salt based composite phase change materials for medium and high temperature thermal energy storage: from component to device level performance through modelling," *Renewable Energy*, vol. 140, pp. 140–151, 2019.
- [19] W. C. Li, Y. F. Cai, and T. Y. Yan, "Preparation of sodium acetate trihydrate/expanded graphite composite phase change materials and its heat storage properties," *Journal of Shanghai Jiaotong University*, vol. 54, no. 10, pp. 1015–1023, 2020.
- [20] S. Hhleln, A. Knig-Haagen, and D. Brüggemann, "Macro-encapsulation of inorganic phase-change materials (PCM) in metal capsules," *Materials*, vol. 11, no. 9, 2018.
- [21] Y. C. Zhang, Y. Wang, J. H. Zhou, Z. R. Zhang, and T. Li, "Preparation and characterization of phase change energy storage wall materials based on desulfurization gypsum," *New Building Materials*, vol. 47, no. 4, pp. 135–146, 2020.
- [22] B. Beyhan, K. Cellat, Y. Konuklu et al., "Robust micro-encapsulated phase change materials in concrete mixes for sustainable buildings," *International Journal of Energy Research*, vol. 41, no. 1, pp. 113–126, 2017.
- [23] Y. W. Wang and W. L. Li, "Preparation and properties of shaped PEG/SiO₂/graphite composite phase change thermal regenerative concrete," *Concrete & Cement Products*, vol. 3, pp. 65–69, 2020.